VOCl as Cathode for Rechargeable Chloride Ion Batteries**

Ping Gao,[a] M. Anji Reddy,[a] Xiaoke Mu,[a, b] Thomas Diemant,[c] Le Zhang,[a] Zhirong Zhao-Karger,[b] Venkata Sai Kiran Chakravadhanula,[a, b] Oliver Clemens[b, d] R. Jürgen Behm,[a, c] and Maximilian Fichtner[a, b,*]

Abstract: A novel room temperature rechargeable battery with VOCl cathode, Li anode and chloride ion transporting liquid electrolyte is described here. The cell is based on the reversible transfer of chloride ions between the two electrodes. The VOCl cathode delivered an initial discharge capacity of 189 mAh g^{-1}. A reversible capacity of 113 mAh g^{-1} was retained even after 100 cycles when cycled at a high current density of 522 mA g^{-1}. For the first time such high cycling stability was achieved in chloride ion batteries demonstrating the practicality of system beyond the proof-of-concept. The electrochemical reaction mechanism of the VOCl electrode in the chloride ion cell was investigated in detail by ex-situ X-ray diffraction (XRD), infrared spectroscopy (FTIR), transmission electron microscopy (TEM) and X-ray photoelectron spectroscopy (XPS). The result confirms reversible deintercalation/intercalation of chloride ions in the VOCl electrode.

Recently, a novel rechargeable battery has been demonstrated based on chloride shuttle at room temperature.[1] Selected electrochemical couples of this chloride ion battery (CIB) offer theoretical energy densities up to a value of 2500 Wh L^{-1}.[1,2] In principle, various metals with low reduction potential such as Li, Mg, Ca can be used as anode materials for this system. In our previous study, Li and Mg metals were used as anodes for chloride ion battery cells with different cathode materials.[1-4] In the first study of a CIB by Zhao *et al.*,[1] using $BiCl_3$, VCl_3 and $CoCl_2$ cathodes, the proof-of-principle was demonstrated and these electrodes exhibited an interesting electrochemical performance for the rechargeable batteries. Also metal oxychlorides such as FeOCl, BiOCl and VOCl have been proposed as potential cathode materials for the CIBs.[2-4] The cathodic and anodic reactions of the CIB during discharge process can be described as follows:

At the cathode: $MClx + xe^- \leftrightarrow M + xCl^-$,

at the anode: $M' + xCl^- \leftrightarrow M'Clx + xe^-$,

where M is the metal (e.g. Fe, Bi or V) or metal monoxide (FeO, BiO or VO) used as cathode and M' is highly electropositive metals (e.g. Li, Mg or Ca) used in the anode. One issue in the first CIB that has been recognized was the dissolution of certain metal chlorides in the electrolyte, which could cause a poor electrochemical performance. The investigation of CIB currently focuses on the exploration of potential electrodes or electrode combinations with high reversibility as well as compatible electrolytes. Ionic liquids were used as electrolytes in previous studies, but also other non-aqueous electrolytes based on carbonate solvent can be used in CIBs, as will be shown. In the following, we report a novel room temperature chloride ion battery (Li / $PP_{14}Cl$-PC / VOCl) by using a VOCl electrode as cathode, lithium metal as anode, and a solution of 0.5 M 1-butyl-1-methylpiperidinium chloride ($PP_{14}Cl$) in propylene carbonate (PC) as an electrolyte. In addition, the electrochemical results of Li/$PP_{14}Cl$-PC/VOCl cell was compared with that of a Li ion cell built with the same cathode and anode, but with a $LiPF_6$ based electrolyte.

VOCl was synthesized by a solid-gas reaction as described in previous work.[4] Typical synthesis was done by heating a 1:1.8 molar ratio of V_2O_3 (98 %, Sigma-Aldrich) and VCl_3 (97 %, Sigma-Aldrich) in an evacuated and sealed quartz tube kept at a temperature of 893 K for 120 h with a heating rate of 1 K min^{-1}. The resulting brown VOCl material was washed with water and acetone to remove the residual VCl_3. The layered VOCl crystallizes in an orthorhombic structure with a space group of *Pmmn* (lattice parameter: *a* = 3.78 Å, *b* = 3.30 Å, *c* = 7.91 Å).[5] The buckled V-O bilayer is sandwiched between chlorine layers which are weakly coupled through van der Waals forces along the crystallographic *c* direction.[6]

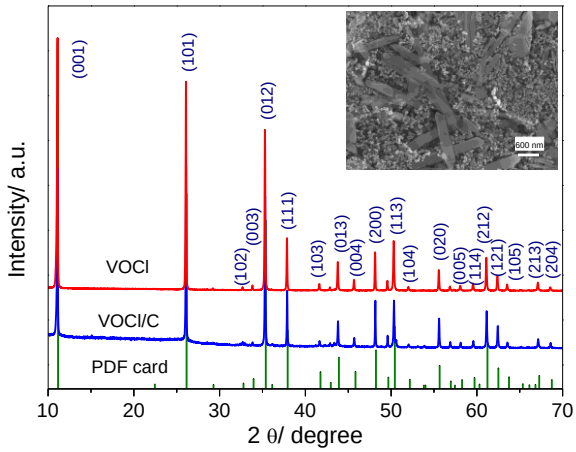

Figure 1. XRD patterns of VOCl and VOCl/C composite, (inset) SEM image of the VOCl/C composite. For a plot of the Rietveld analysis, see the Supporting Information (Figure S1 and Figure S2).

The XRD pattern of the as synthesized VOCl is given in Figure 1. All peaks matched well with the VOCl reference pattern from

[a] P. Gao, Dr. M. A. Reddy, Dr. X. Mu, L. Zhang, Dr. S. K. Chakravadhanula, Prof. Dr. R. J. Behm, Prof. Dr. M. Fichtner
Department Helmholtz Institute Ulm for Electrochemical Energy Storage (HIU), Helmholtzstr.11, D-89081 Ulm, Germany
E-mail: m.fichtner@kit.edu Tel:+49(0)731 5034201. Fax: +49(0)721 6086368 (M.F.).

[b] Dr. X. Mu, Dr. Z. Z. Zhao-Karger, Dr. S. K. Chakravadhanula, Dr. O. Clemens, Prof. Dr. M. Fichtner
Institute of Nanotechnology, Karlsruhe Institute of Technology (KIT), P.O.Box 3640, D-76021 Karlsruhe, Germany

[c] Dr. T. Diemant,, Prof. Dr. R. J. Behm
Institute of Surface Chemistry and Catalysis, Ulm University, Albert-Einstein-Allee 47, D-89081 Ulm, Germany

[d] Dr. O. Clemens
Joint Research Laboratory Nanomaterials, Jovanka-Bontschits-str. 2, Darmstadt University of Technology, D-64287 Darmstadt, Germany

Supporting information for this article is given via a link at the end of the document.

PDF card no. 01-074-1274. In addition, we found small amounts of impurity phases of V_2O_3 (~ 2 wt %), VCl_2 (~ 1 wt %), and, presumably, an fcc metal, which were found to be unaffected by subsequently performed discharging / charging cycles (Figure S2) showing their electrochemical inactivity. Figure S3 shows the SEM images of as-synthesized VOCl particles. They exhibit a rod shape morphology with a length of 2 - 5 µm and ~ 300 nm diameter. As VOCl is a semiconductor,[7–9] it was mixed with carbon black as conducting additive using mortar and pestle in order to provide good electrical contact of VOCl in the electrode. The inset in Figure 1 shows that the VOCl particles were homogenously dispersed in the carbon black, and they retained the same morphology and particle size as the pure VOCl material shown in Figure S3.

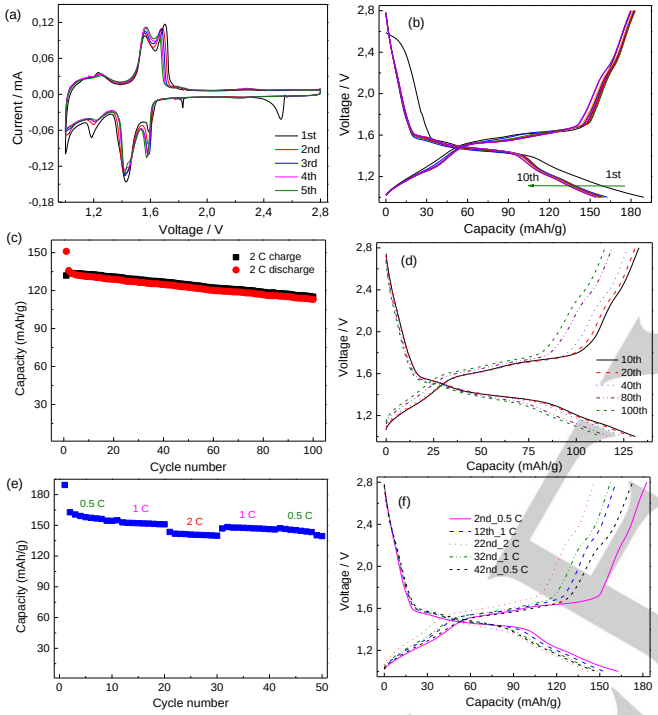

Figure 2. (a) CV curves of Li / PP_{14}Cl-PC / VOCl cell at a scan rate of 0.1 mV s^{-1}, (b) initial charge/discharge curves of the cell at 0.5 C in the voltage range of 1.0 - 2.8 V. Cycling performance at 2 C (c, d) and rate performance (e, f) of the Li / PP_{14}Cl-PC / VOCl cell.

The liquid electrolyte of PP_{14}Cl-PC (0.5 M) prepared in this study has a high ionic conductivity of 4.4 mS cm^{-1} with an electrochemical window of 3.2 V versus lithium metal measured at room temperature (Figure S4), which is enough to provide a stable environment for the electrochemical reaction. The initial CV curves of Li / PP_{14}Cl-PC / VOCl cell scanned at 0.1 mV s^{-1} in the voltage range of 1.0 - 2.8 V and 0.5 - 3.0 V are shown in Figure 2a and Figure S5, respectively. Three main redox couples were observed at 1.57/1.67 V, 1.42/1.56 V, and 1.2/1.26 V in a voltage range of 1.0-2.8 V, which indicates a multi-step reaction proceeding during the discharge and recharge process. A structural model for such stepwise behavior reaction is proposed in the supporting information. In the subsequent cycle, CV curves were similar to that of the first one, which demonstrates the reversibility of the electrochemical process. In addition, an irreversible anodic peak was observed at around 2.5 V in the first cycle. The origin of this peak will be discussed below. Figure 2b shows the discharge and charge curves of the Li / PP_{14}Cl-PC / VOCl cell for the first 10 cycles obtained at a rate of 0.5 C (1 C = 261 mA g^{-1}) at 298 K. A small plateau was observed at 2.5 V, then the voltage dropped monotonically to 1.7 V and three discharge plateaus were observed at around 1.6, 1.5 and 1.2 V. The corresponding differential capacity plots are shown in Figure S6, giving similar peaks as observed in the CV measurement. The cell delivered a total discharge capacity of 189 mAh g^{-1} in the 1st discharge, corresponding to 0.72 electrons per VOCl unit participating in the reaction. A capacity of 180 mAh g^{-1} was recovered in the first recharge process with an irreversible capacity loss (ICL) of 9 mAh g^{-1} at 0.5 C in the first cycle. Subsequent discharge and charge curves were similar to the first discharge and charge, indicating a high reversibility of the VOCl electrode in this battery.

The length of the small plateau at 2.5 V corresponds to a capacity of 20 mAh g^{-1}, which is equivalent to 0.07 mole electron transfer. This step is attributed to the intercalation of PP_{14} ions from the electrolyte into the VOCl electrode. It was shown before that large organic cations can be intercalated into the interlayer of metal oxychlorides.[10–14] The intercalated molecule has in fact been detected by combined XRD, FTIR and XPS measurements, which will be discussed later.

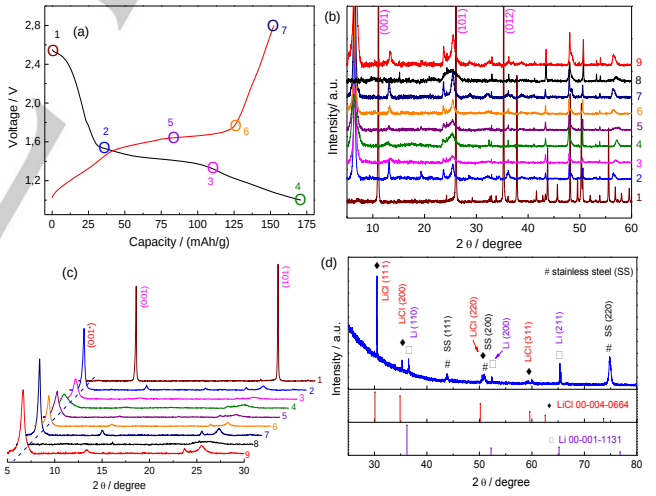

Figure 3. (a) Charge/discharge curve of the VOCl electrode at 1 C in the first cycles.The different electrochemical states at which *ex-situ* XRD measurement were performed are marked. (b and c) *Ex-situ* XRD patterns of VOCl electrode at different charge/discharge states in the 1st cycle and 10th cycle and (d) XRD patterns of lithium anode after the first discharge.

The cycling performance of Li / PP_{14}Cl-PC / VOCl operated at a current density of 2 C is given in Figure 2c. A first discharge capacity of 151 mAh g^{-1} was obtained in the voltage range of 1.0 - 2.8 V. Then the capacity faded to 135 mAh g^{-1} in the 2nd cycle and a capacity of 113 mAh g^{-1} was obtained after 100 cycles with a coulombic efficiency of 98 %. The polarization increased slightly during the cycling as shown in Figure 2d. The rate

performance of the Li / $PP_{14}Cl$-PC / VOCl battery is shown in Figure 2e. Discharge capacities of 189 mAh g^{-1}, 154 mAh g^{-1} and 143 mAh g^{-1} were obtained at 0.5 C (1st), 1 C (11th) and 2 C (21st) rate, respectively. After 10 cycles at 2 C, the discharge capacity of 148 mAh g^{-1} (1 C, 32nd) and 147 mAh g^{-1} (0.5 C, 42nd) can be recovered in the subsequent cycling. This demonstrates that the cell could deliver a high rate capacity combined with a decent cycling stability. The charge and discharge curves of the VOCl electrode cycled at different current densities are given in Figure 2f, where a quite similar curve with slight increase of the polarization was observed at a high current density.

In order to understand the reaction mechanism of the Li / $PP_{14}Cl$-PC / VOCl battery, *ex-situ* XRD of the VOCl electrode and lithium anode was performed at different electrochemical states in the 1st and 10th cycle to investigate the phase evolution during the electrochemical reaction (Figure 3). Figure 3a shows the discharge and charge curve of the VOCl electrode for the first cycle at 1 C with seven discharged and charged states where *ex-situ* XRD measurements were made. In the 1st cycle, point 1 to point 7 represent the VOCl electrode in the electrochemical state of as-prepared (1), discharged 1.53 V (2), discharged 1.33 V (3), discharged 1.0 V (4), recharged 1.62 V (5), recharged 1.75 V (6) and recharged 2.8 V (7), respectively. Point 8 and point 9 shown in Figure 3b and 3c represent the discharged 1.0 V and recharged 2.8 V of the VOCl electrode in the 10th cycle. Figure 3b shows the full XRD pattern and Figure 3c shows the selected XRD patterns at low angles, respectively. After discharging to 1.53 V (point 2), the XRD pattern was significantly different from that of the as-prepared VOCl electrode, particularly in the low angle region as shown in Figure 3b and 3c. A new strong reflection evolved at $2\theta = 6.5°$, which corresponds to a d spacing value of 13.38 Å. Compared to the original VOCl with the *c* axis spacing of 7.91 Å, an expansion by 5.47 Å took place, which is an indication for the intercalation of 1-butyl-1-methylpiperidinium cation (PP_{14}^+) between the VOCl interlayers during the initial stage of discharge. The PP_{14}^+ molecule is illustrated in Figure S7, it is expected that the molecule prefers an orientation horizontal to the host. Expansion of MOCl layers upon intercalation of large organic cations were also noticed in other metal oxychlorides such as, FeOCl,[10-13] TiOCl[14] and VOCl.[14,15] All further reflections at higher angles strongly decrease in intensity, which is indicative for strong increasing disorder (potentially resulting from relative torsion of neighbouring layers or buckling of layers, with relative reorientations of neighboring layers being a well-known phenomenon of this structure type).[12,16,17] The analysis of the patterns in the charged and discharged state is provided in the supporting information. Upon further discharge to point 3 and point 4, the reflections which must be assigned to the VOCl type phase show increased broadening. Interestingly, upon recharging to 2.8 V (point 7), the initial width is gradually recovered, demonstrating a topotactic nature of the electrochemical reaction (see supporting information for a more detailed explanation). In the discharge state of the 10th cycle (Figure 3b and 3c, point 8), (00l) type reflections show an extremely strong increase of broadening, with the remaining part of the pattern being rather similar to previous charge/discharge states. However, in the subsequent recharge (point 9), all peaks were recovered and the XRD pattern was in good agreement with the pattern recorded in the 1st cycle (point 7). Again, this is in good agreement with the observed topotactic nature of the reaction, and hints at strong influences on the crystallinity/disorder within the compound by increasing the cycle number. In Figure 3(c), the sharp reflections observed in XRD patterns 2-9 belong to impurity phases (a fit of the diffraction data of point 7 is shown in Figure S8) also found for the state 1, but better visible than for diffraction pattern 1 due to the strong decrease of overall intensity.

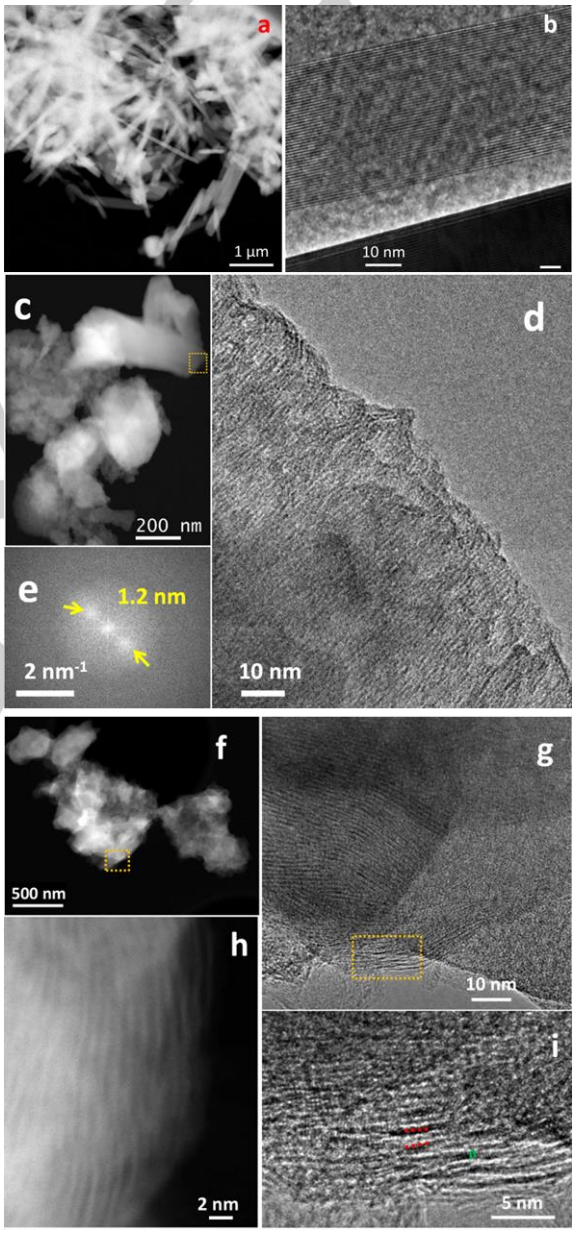

Figure 4. (a) STEM-HAADF large-area image and (b) enlarged HRTEM micrograph of the as-prepared VOCl. (c) STEM-HAADF overview image of the discharged sample, (d) low-dose HRTEM micrograph from the area indicated in c, (e) fast Fourier transform of the HRTEM image in c, where the yellow arrows highlight the reflections corresponding to $(001)_{VOCl}$. (f) STEM-HAADF overview image of the recharged sample, (g) HRTEM micrograph from the area indicated in f, (i) magnified image of marked area in g, where the red dot-

lines highlight distorted (001) lattices with a d-value of ~1.2 nm (h) STEM-HAADF image from the same area as i showing the distorted (001) lattices.

The lithium anode was also tested by *ex-situ* XRD to further understand the phase evolution in the first discharge as shown in Figure 3d. Reflections at 2θ = 30.4°, 35.2° and 50.3°, related to LiCl (PDF card no.00-004-0664), were detected as well as the lithium phase (2θ = 36.2°, 52.1° and 65.2°, PDF card no. 00-001-1131) and the stainless steel current collector (2θ = 43.8°, 50.9° and 74.9°). This demonstrates that the lithium anode was oxidized to form LiCl by taking chloride ions transported through the electrolyte during the discharge. The Cl/V ratio from the SEM-EDX spectra measured at several particles of the VOCl electrodes after the first cycle (Figure S9) evidences a loss and gain of chloride in the discharge and recharge process. Taken together, the voltage composition profiles and *ex-situ* XRD results demonstrate that the discharge and charge reaction mechanism in the first and subsequent cycles is the same.

Figure 4a shows a STEM-HAADF overview image of the rod-shape morphology in the as-prepared sample. The HRTEM micrograph (Figure 4b) reveals the layered structure corresponding to the van der Waals bonded $(001)_{VOCl}$ planes. In the discharged state, the HRTEM micrograph (Figure 4d) shows layered features and the corresponding fast Fourier transformation (FFT) (Figure 4e, highlighted by the arrows) exhibits broad peaks with 1.2 nm lattice distance, corresponding to a distorted $(001)_{VOCl}$ lattice, in agreement with the XRD results in Figure 3b. Figure S10 demonstrates that the discharged sample is sensitive to electron beam damage. 2 ~ 3 nm vanadium (III) oxide crystallites with space group of Fm3m (225) form under electron beam irradiation of the experiment (approximately 5×10^7 electrons nm^{-2}).[18] This result indicates the meta-stability of the layered structure in the discharged sample in contrast to the as-prepared and recharged sample. The d-values determined from the STEM-HAADF and the HRTEM micrographs of the recharged sample (Fig. 4g, h and i) correspond to the distorted reflection of the $(001)_{VOCl}$ lattice plane. The TEM mapping of the discharged and recharged VOCl electrodes are shown in Figure S11 and S12, respectively. Figure 5a shows EEL spectra recorded on the same area of the TEM for the as-prepared (solid, black), discharged (dash-dotted, red) and recharged (dotted, blue) samples including the Cl-L edge at 200 eV and the V-L edge at 512 eV. The three (background corrected) spectra are aligned with respect to the vanadium signal. The area under the Cl-L edge directly relates to the relative amount of Cl in the three samples, implying a loss and gain of chloride ions in the VOCl electrode during the discharge and recharge process, respectively.

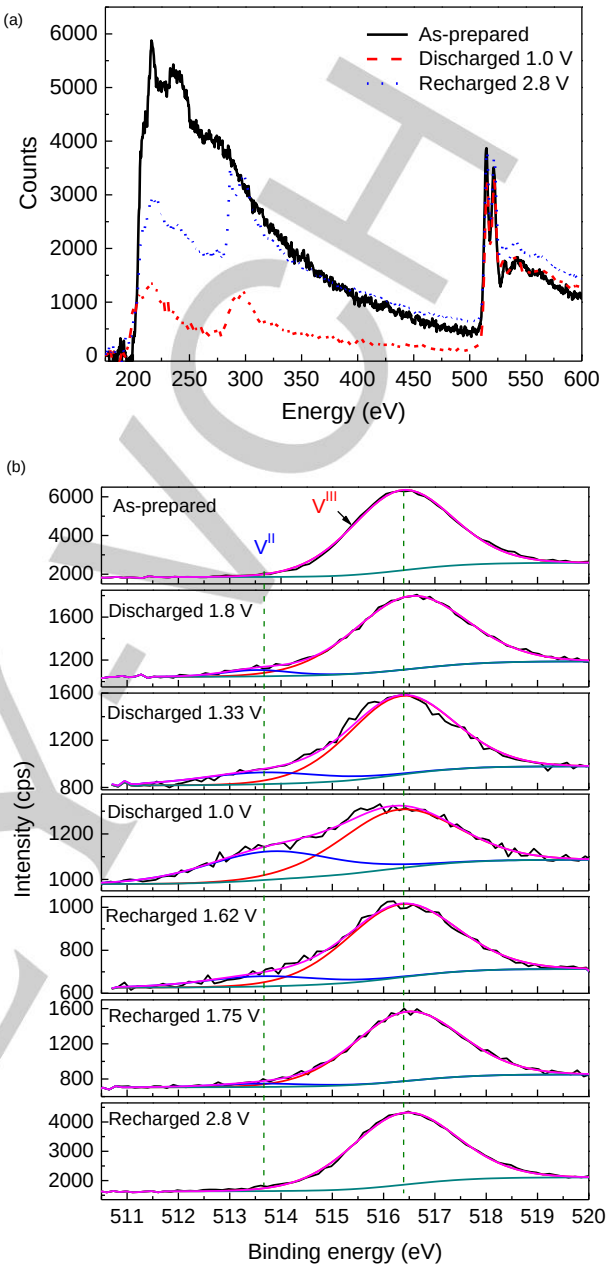

Figure 5. (a) EEL spectra of the as-prepared (black, solid line), discharged (red, dashed line) and recharged (blue, dotted line) samples. The features at 285 eV are due to the carbon K edge from the binder. The spectra are vertically aligned with respect to the background subtracted vanadium peak. (b) XPS spectra in the $V_{2p3/2}$ region of VOCl electrodes in various electrochemical states.

The oxidation state of vanadium in different electrochemical states was investigated by *ex-situ* XPS measurements to further understand the reaction mechanism of the Li / $PP_{14}Cl$-PC / VOCl. Figure 5b shows the XP spectra of the $V_{2p3/2}$ regions in the as-prepared, discharged to 1.8 V, 1.33 V, 1.0 V, and recharged to 1.62 V, 1.75 V, 2.8 V states of the VOCl electrode for the 1st cycle. The survey spectra of the electrode at these points are given in Figure S13. In the as-prepared sample, a single peak

was observed in the $V_{2p3/2}$ region with a binding energy of 516.3 eV, which can be ascribed to the trivalent vanadium in VOCl.[19] Upon discharging to 1.8 V, a new peak with a binding energy of 513.7 eV appeared, in addition to the $V_{2p3/2}$ peak at 516.3 eV, which is attributed to the $V_{2p3/2}$ state in V^{2+}.[20] The peak area attributed to V^{2+} (it is not large which may be due to its sensitivity on the surface) increased generally upon discharge and decreased during the recharge process again. In the recharged VOCl (2.8 V), the lower binding energy peak disappeared and only the peak at 516.4 eV was left, demonstrating that the V^{2+} was transformed back into V^{3+} in the recharge process. The observation of vanadium in a lower chemical valence can be ascribed to the partial reduction of V^{3+} to V^{2+}, in accordance to the dissociation of chloride ions from the VOCl in the discharge process. After recharging, the V^{3+} was re-gained in VOCl, which demonstrates a reversible oxidation-reduction process. In addition, XP spectra of the Cl_{2p} region of these VOCl electrodes and from lithium anodes in different states are shown in Figure S14 and S15, respectively.

To gain further insight into the potential intercalation of the organic cation from $PP_{14}Cl$ into VOCl, we performed additional IR, XPS, and SEM measurements. The discharged electrode was washed several times by PC and DMC, to remove any precipitated $PP_{14}Cl$ on the surface of the electrode. Figure S16 shows the FTIR spectra of the PVDF, VOCl after discharge to 1.33 V and 1-butyl-1-methylpiperidinium chloride ($PP_{14}Cl$). The FTIR of the VOCl in different electrochemical states and the assignment of the peaks are shown in Figure S17, S18 and Table S1. The bands at 944, 2872 and 2938 cm^{-1} are assigned to the N-C (CH_3) stretching and the twisting / rocking of H-C-H in the piperidinium ring, the symmetric and asymmetric C-H stretching in the butyl group and in the piperidinium ring, respectively.[21] A shift of the bands to lower frequency at 921, 2866 and 2920 cm^{-1} was observed in charged/discharged samples which is in agreement with analogue layered material intercalated with guest molecules,[16] suggesting the intercalation of PP_{14} cation in the interlayer of VOCl. Figure S19 shows the N_{1s} XP spectra of the VOCl electrode in the as-prepared and in the discharged to 1.8 V, 1.33 V and recharged to 1.62 V, or 1.75 V states. The appearance of the N_{1s} peak after discharging to 1.8 V and its persistence during recharging further demonstrates the intercalation of the PP_{14} cation into the VOCl electrode. In addition, an expansion of the layered structure of the discharged VOCl electrode was also observed by SEM as shown in Figure S20. Based on the above observations and the XRD results, we conclude that the cation of $PP_{14}Cl$ molecule is intercalated into the layered VOCl material during the initial stage of the first discharge and remains intercalated during further cycles.

Based on the electrochemical, *ex-situ* XRD, TEM, FT-IR and XPS analysis we postulate the following mechanism for the Li / $PP_{14}Cl$-PC / VOCl cell. During the initial discharge at 2.5 V, 0.07 mol of the PP_{14} cation are intercalated irreversibly into the VOCl electrode, leading to an expansion of the layers. For charge balancing, an equal amount of Cl^- ions reacts with the anode and forms LiCl. Upon further discharge, chloride ions are deintercalated from VOCl, transported through the electrolyte, and react with Li to form LiCl. During the recharge process the chloride ions are intercalated into the VOCl electrode. The intercalated PP_{14} cation facilitates the chloride deintercalation and intercalation process by keeping the layers wide and intact, which is evidenced by the reversible change of width of the peak at $2\theta = 6.5°$ during discharge and charge. This could be the reason for the good reversible capacity of the electrode observed also for high current densities. The proposed reaction mechanism and the detailed explanation for the reaction are outlined in further detail in the supporting information.

It is interesting to compare the discharge profiles of the Li / $PP_{14}Cl$-PC / VOCl and Li / $LiPF_6$-EC-DMC-PC / VOCl cell, the former based on chloride ion transport and the later based on lithium-ion transport, see Figure S21. The discharge and charge profiles of the cell based on lithium ion transport are completely different and give further evidence that the Li / $PP_{14}Cl$-PC / VOCl cell works by a different mechanism. However, in the chloride ion cell, the discharge product of LiCl, even with a low solubility in PC solvent, may dissolve to a certain extent. Therefore, the interference of lithium intercalation into VOCl electrode cannot be ignored during long cycling.

In summary, we have presented a novel room temperature Li / $PP_{14}Cl$-PC / VOCl chloride ion battery using VOCl as cathode, lithium foil as anode and 1-butyl-1-methylpiperidinium chloride dissolved in propylene carbonate solvent as electrolyte. The reversible behavior of the Li / $PP_{14}Cl$-PC / VOCl cell was characterized by CV and galvanostatic measurements. The results show that the battery can be well discharged and recharged even at a high current density. The cell shows a first discharge capacity of 189 mAh g^{-1} at 0.5 C, corresponding to 0.72 mol of electrons transferred in the reaction. A discharge capacity of 113 mAh g^{-1} was obtained at 2 C with a coulombic efficiency of 98 % during 100 cycles. The mechanism of the Li / $PP_{14}Cl$-PC / VOCl chloride ion battery was validated by *ex-situ* XRD, TEM, FTIR and XPS measurements. The results indicated that the chloride ion indeed shuttles between the cathode and anode.

Acknowledgements

Financial support from China Scholarship Council (CSC) (P.G.) and through the EU project Hi-C in FP 7, grant # 608575, (X.M) is gratefully acknowledged. The authors thank Nina Laszczynski, Helmholtz Institute Ulm, for the lithium anode XRD measurement and the Helmholtz large scale user facility Karlsruhe Nano Micro Facility (KNMF) for access to the TEM. C.V and X. M thank Dr. Christian Kübel and Prof. Dr. Horst Hahn for their continuous support.

Keywords: chloride ion battery • electrochemistry • rechargeable • vanadium oxychloride

[1] X. Zhao, S. Ren, M. Bruns, M. Fichtner, *J. Power Sources* **2014**, *245*, 706-711.

[2] X. Zhao, Z. Zhao-Karger, D. Wang, M. Fichtner, *Angew. Chem. Int. Ed. Engl.* **2013**, *52*, 13621-13624.

[3] X. Zhao, Q. Li, Z. Zhao-Karger, P. Gao, K. Fink, X. Shen, M. Fichtner, *ACS Appl. Mater. Interfaces* **2014**, *6*, 10997-11000.

[4] P. Gao, X. Zhao, Z. Zhao-Karger, T. Diemant, R. J. Behm, M. Fichtner, *ACS Appl. Mater. Interfaces* **2014**, *6*, 22430-22435.

[5] H. Schaefer, F. Wartenpfuhl, *J. less-common Met.* **1961**, *3*, 29-33.

[6] N. A. Bogdanov, J. Van Den Brink, L. Hozoi, *Phys. Rev. B* **2011**, *84*, 235146-6.
[7] S. Glawion, M. Scholz, Y.-Z. Zhang, R. Valentí, T. Saha-Dasgupta, M. Klemm, J. Hemberger, S. Horn, M. Sing, R. Claessen, *Phys. Rev. B* **2009**, *80*, 155119.
[8] E. Benckiser, R. Rückamp, T. Möller, T. Taetz, A. Möller, A. A. Nugroho, T. T. M. Palstra, G. S. Uhrig, M. Grüninger, *New J. Phys.* **2008**, *10*, 1-21.
[9] P. Palvadeau, D. Schleich, J. Rouxel, *Mat.Res.Bull.* **1979**, *14*, 891-897.
[10] J. F. Bringley, B. A. Averill, *Chem. Mater.* **1990**, *2*, 180-186.
[11] J. F. Bringley, Jean-Marc Fabre, B. A. Averill, *J. Am. Chem. Soc.* **1990**, *112*, 4577-4579.
[12] S. M. Kauzlarih, J. L. Stanton, J. Faber, B. A. Averill, *J. Am. Chem. Soc.* **1986**, *108*, 7946-7951.
[13] R. H. Herber, Y. Maeda, *Inorg. Chem.* **1981**, *20*, 1409-1415.
[14] I. Kargina, D. Richeson, *Chem. Mater.* **1996**, *8*, 480-485.
[15] S. Clough, P. Palvadeau, J. P. Venien, *J. Phys. C: Solid State Phys.* **1982**, *15*, 641-655.
[16] L. Cario, S. Delagrange, F. Boucher, E. Faulques, P. Palvadeau, *Chem. Mater.* **2003**, 15, 4325-4331.
[17] J. E. Phillips, R. H. Herber, *Inorganic Chemistry*. **1986**, 25, 3081-3088.
[18] N. Schönberg, W. G. Overend, A. Munthe-Kaas, N. A. Sörensen, *Acta Chem. Scand.* **1954**, *8*, 221-225.
[19] M. Demeter, M. Neumann, W. Reichelt, *Surf. Sci.* **2000**, *454-456*, 41-44.
[20] E. Hryha, E. Rutqvist, L. Nyborg, *Surf. Interface Anal.* **2012**, *44*, 1022-1025.
[21] M. Shukla, H. Noothalapati, S. Shigeto, S. Saha, *Vib. Spectrosc.* **2014**, *75*, 107-117.

COMMUNICATION

A highly reversible rechargeable chloride ion battery is reported. The battery is based on the reversible transfer of chloride ions between the VOCl cathode and the lithium anode. A reversible capacity of 113 mAh g^{-1} can be retained after 100 cycles even at a high current density of 2 C rate.

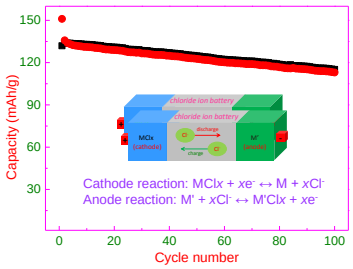

*Ping Gao, M. Anji Reddy, Xiaoke Mu, Le Zhang, Zhirong Zhao-Karger, Venkata Sai Kiran Chakravadhanula, Thomas Diemant, R. Jürgen Behm, and Maximilian Fichtner**

Page No. – Page No.
Electrochemical Investigation of VOCl for Rechargeable Chloride Ion Batteries